

Fig. 7. Same as Fig. 3, except that calculations are based on nearest-neighbor interactions for the case of $\{112\} \langle 111 \rangle$ slip.

those of Table I) are listed in Table III. It may be noted that in determining the operating slip systems for a given crystal orientation, an equivalent Bishop and Hill method has not been developed for $\{112\} \langle 111 \rangle$ slip. The procedure used here is based on the principle of minimum shear adopted by Taylor¹⁵, the results of which are equivalent to the Bishop and Hill method. In the Taylor method, various combinations of glide-shears (from different slip systems) which satisfy the imposed (rolling) strain are obtained by trial; the combination(s) selected is one in which the sum of the absolute value of the glide-shears is a minimum. Since the number of slip system combinations is large, no attempt was made here to consider all of them. Instead, a judicious selection of the most likely combinations was tried; hence the results should approximate very closely (if not exactly) to the minimum shear condition*.

The results of the calculations are summarized in Table IV, with the anisotropy energies in the three symmetry directions of a rolled strip plotted in Fig. 7. It can be seen from Fig. 7 that the rolling direction is the highest energy or hardest direction,

* Note added in proof (12-5-66): Since this paper was written, the complete Taylor analysis for $\{112\} \langle 111 \rangle$ slip has been performed by a computer method. The computer results confirmed that the operating slip systems determined by the previous less rigorous method truly conformed to the minimum shear condition. Thus the uncertainties expressed in Section 3(3) are removed. (The author is grateful to Mrs. W. L. Mammel and Mrs. G. Souren for the computer programming.)

as required by the observed results of Fahlenbrach *et al.*

In Fig. 8 we combine Figs. 3 and 7 for the case of mixed $\{110\} \langle 111 \rangle$ and $\{112\} \langle 111 \rangle$ slip, with contributions of 50 and 75% $\{112\} \langle 111 \rangle$ shown. It may be noted that if RD, TD and RPN are to be arranged in the order of decreasing energy as implied by Fahlenbrach's observations, Fig. 8 indicates that more than about 60% of the deformation is taken up by $\{112\} \langle 111 \rangle$ slip. If the weaker NNN interactions (Fig. 4) are included, this value would be somewhat higher.

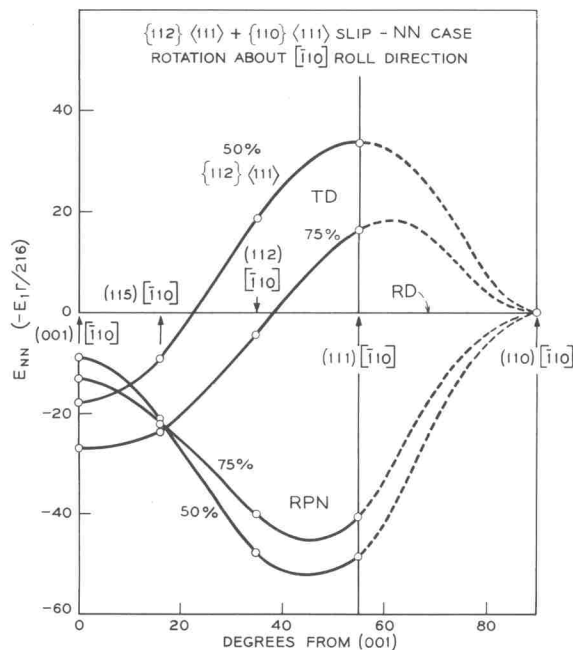


Fig. 8. Figures 3 and 7 combined, for the case of mixed $\{110\} \langle 111 \rangle + \{112\} \langle 111 \rangle$ slip. Curves shown are for 50% and 75% $\{112\} \langle 111 \rangle$ slip. Note that the average energy from (001) $[\bar{1}10]$ to (111) $[\bar{1}10]$ is lowest for RPN, and TD has lower average energy than RD for greater than about 60% $\{112\} \langle 111 \rangle$ slip.

4. DISCUSSION

While the present theory is capable of explaining the observed results in the polycrystalline material, tests on single crystals are less ambiguous. Such tests can be done conveniently with magnetic torque measurements of disks cut out of the rolling plane. Figure 8 shows that in the (001) $[\bar{1}10]$ orientation, RD is a harder direction than TD. As the orientation rotates away, the rolling plane becomes isotropic in the vicinity of (112) $[\bar{1}10]$,

beyond which TD becomes a harder direction. Finally, the rolling plane becomes isotropic again at (110)[$\bar{1}10$]. In these single crystal studies, two points need to be considered. First, because of lattice rotations that may accompany the deformation, the results on heavily rolled samples may need to take into account such changes in crystal orientation. From the polycrystalline texture analogy, the most stable orientations are from (100)[$\bar{1}10$] to (112)[$\bar{1}10$]. Secondly, the analysis is based on plane strain deformation. For some orientations, notably (110)[$\bar{1}10$], the disposition of the slip systems is such that the crystal tends to widen. In this case, ordinary rolling procedures may become inadequate. To insure negligible width change, a better method is to deform the crystal in a simple plane strain compression fixture which consists of a channel formed by die blocks¹⁶. In addition, this method allows a more homogeneous deformation, ready examination of slip lines, and accurate alignment of orientation even for small crystals. The latter feature may be especially important in FeCo, where the α - γ solid state transformation has so far prevented successful growing of large single crystals.

The possibility exists, of course, with studies on other ferromagnetic alloys that exhibit the B2 superlattice. Such alloys are few indeed, at least in the binary systems. The alloy FeRh may be the only suitable candidate besides FeCo.

According to Kouvel and Hartelius¹⁷, this alloy undergoes an antiferromagnetic-ferromagnetic transition on heating to about 350°K. The structure in both cases is B2. Except for possible complications from the magnetic transition, there is no reason why slip-induced directional order could not be studied in the ferromagnetic state. Such a study should reveal the sign of the coefficient l of the pseudo-dipolar coupling energy (see eqn. (1)) for FeRh.

A further note regarding the present theory concerns the possible developments of other types of magnetic anisotropy during rolling. One of these is the magnetocrystalline anisotropy. Since preferred orientation is obtained on rolling, crystal anisotropy could be a factor. The results on the 2% V-FeCo alloy⁶ indicate that the cold-worked induced anisotropy almost disappears after annealing at 500–600°C. Since the recrystallization temperature for this alloy is about 700°C*, the deformation texture is not expected to change after such an anneal. On the other hand, it prob-

ably converts the disordered (cold-worked) matrix to a long-ranged ordered state. According to Hall²¹, the crystal anisotropy constant $K_1 \approx -2 \times 10^5$ ergs/cm³ for the disordered alloy and decreases with ordering, which could then explain the corresponding decrease of the observed anisotropy after the 500–600°C anneal. However, a large negative value of K_1 in the cold-rolled state implies the $\langle 111 \rangle$ direction as the easy axis of magnetization. There is then difficulty of explaining why the rolling plane normal, which consists of a rotational spread from {100} to {111} (see Fig. 2), is the especially easy axis as observed. Studies in the vicinity of 42–45% Co, where $K_1 \approx 0$ in the disordered state²¹, should further elucidate the role of crystal anisotropy in rolled material.

A second source of anisotropy in the rolled material is magnetostrictive anisotropy. Because of the large magnetostriction of FeCo, the residual stress that remains after rolling could lead to a substantial magnetostrictive anisotropy energy. The residual stress pattern and its effect on the overall magnetic anisotropy remain unclear. Unless a stress is uniformly directed throughout the material (such as by applying a tensile or compressive force), it is not expected to result in a large overall anisotropy. Experiments indicate that the rolled anisotropy in nickel, a relatively magnetostrictive material, is nil^{22,23} or at most 10^2 ergs/cm³ (ref. 3). Assigning the latter value to magnetostrictive anisotropy and adjusting for the larger magnetostriction in FeCo (2–3 times over Ni), one is still far from the observed anisotropy energy of 10^5 ergs/cm³ observed in rolled FeCo^{7,8}.

SUMMARY

The slip-induced directional order theory has been developed for the B2-type superlattices. The theory is then applied to calculate the magnetic anisotropy obtained by rolling of single crystals near the FeCo composition. The results of analyses on orientations which comprise the crystallographic texture spread of the rolled polycrystalline material are

* Although this temperature was actually obtained with the binary FeCo alloy^{18,19}, no appreciable change from the small vanadium addition is expected. According to English²⁰, the ordering reaction, which appears responsible for the high recrystallization temperature of FeCo^{18,19}, is essentially complete after a few seconds of annealing at 565°C in the 2% V-FeCo alloys.